SCIENCE CHINA
Information Sciences

• **RESEARCH PAPER** •
Special Focus on High-Speed Signal Processing

February 2015, Vol. 58 020302:1–020302:10
doi: 10.1007/s11432-014-5240-3

Compressed sensing digital receiver and orthogonal reconstructing algorithm for wideband ISAR radar

HOU QingKai*, LIU Yang, FAN LiJie & SU ShaoYing

National University of Defense Technology, Changsha 410073*, China*

Received August 10, 2014; accepted October 27, 2014

Abstract This paper proposes a novel design of intermediate frequency (IF) digital receiver for wideband inverse synthetic aperture radar (ISAR) based on compressed sensing (CS). For the convenience in engineering application, we use random sampling in the digital receiver and make it possible to digitize the wideband IF signal using a commercial off-the-shelf analog-to-digital converter with sub-Nyquist sample rate. Besides, a novel basis for the sparse representation of real-valued ISAR radar echoes is built in this paper, and an orthogonal CS reconstructing algorithm is proposed based on this. Using our proposed method, the complex-valued range profile of target can be directly reconstructed from the subsampled real raw echo. The phase information of target range profile, which is very important for the coherent processing in ISAR imaging, is well reserved during the reconstruction. As a result, the down converter and matched filter, which are essential in conventional radar receiver, can be eliminated in our CS digital receiver. A series of simulation validates our design and demonstrates the feasibility of the sub-Nyquist sampling. The simulation results of ISAR imaging verify the validity and superiority of the proposed orthogonal reconstructing method.

Keywords compressed sensing, ISAR imaging, digital receiver, random sampling, orthogonal receiver

Citation Hou Q K, Liu Y, Fan L J, et al. Compressed sensing digital receiver and orthogonal reconstructing algorithm for wideband ISAR radar. Sci China Inf Sci, 2015, 58: 020302(10), doi: 10.1007/s11432-014-5240-3

1 Introduction

Due to the development of software radio, digital radar has become an emerging trend and is treated as the next generation of radar [1–3]. Digital receiver is the key technique in the design of digital radar, and the growth of digital technology is pushing analog-to-digital converter (ADC) closer and closer to the antenna. Digital receiver directly samples the intermediate frequency (IF) or even radio frequency signal and has been proved to own much higher stability and more flexibility than conventional analog receiver [4]. Most of the existing digital receivers use band-pass sampling when digitizing the radar echoes. Band-pass sampling is a special case in the frame of Shannon Nyquist sampling theory. It requires that the sampling rate must be at least two times of the bandwidth of the analog signal [5]. However, ultra wideband radars such as synthetic aperture and inverse synthetic aperture radars often employ signal with pretty wide bandwidth to obtain enough range resolution [6,7]. It is pretty expensive and complicated to sample the wideband echo signal using off-the-shelf ADCs. Even if the band-pass sampling is achievable,

* Corresponding author (email: houkai07@126.com)

the ultra high-speed sampling generates too many sample results, making it incredibly difficult for data storage or transmission.

Recent theory of compressed sensing (CS) proves that if a signal is sparse in some basis or transform domain, it can be captured with far fewer measurements than Nyquist criteria and recovered with overwhelming probability using some optimization algorithms [8]. Some researchers in Rice University have extended the CS to analog signals and developed a framework for analog-to-information conversion. They suggest that if the information level of the signal is lower than the actual bandwidth, it can be sampled at a sub-Nyquist rate and the information of interest will be reconstructed afterward [9].

Great attention has been attracted to applying CS in various radar tasks. The application of CS into ISAR imaging radar is one of the hot spots recently, because the targets of ISAR radar often show sparse reflections in the scene of radar and occupy only a few pixels in the images [10,11]. A lot of attempts have been undertaken to use CS to achieve equivalent effect with less measurement [11–14]. Most of the researches focus on the sparse sampling in the slow time or in the azimuth domain [15,16]. As we mentioned before, sampling and digitizing wideband radar signal is very difficult in the architecture of Nyquist sampling, so we believe that it is quite promising and interesting to apply CS in the acquisition of wideband radar signal.

In this paper, we aim at designing a digital receiver for wideband ISAR radar using state-of-the-art ADC, which is convenient for engineering implementation. A CS solution is proposed to sample the echoes at sub-Nyquist rate and the amount of sampled data can be reduced sharply. We first provide the basics of CS theory and describe the sparse representation of ISAR radar echo in Section 2. In Section 3, a feasible architecture to implement the CS digital receiver for IF signal of wideband ISAR radar is presented. In Section 4, a novel algorithm is proposed to process the subsampled real-valued signal. The complex-valued range profile of target can be reconstructed using our method, and the phase information is well reserved during the recovery. In Section 5, some experiments are provided to evaluate the performance of our design and algorithm in reconstructing the range profile and ISAR image from subsampled data. Both simulated data and actual measured radar echoes are used in our experiments. Section 6 is dedicated to the conclusion.

2 Sparse representation of ISAR radar echo

According to the theory of CS, a sparse representation of signal must be built before reconstructing it by CS method. So, we first discuss the sparsity of ISAR radar echo. Suppose a monostatic, single-pulse, and far-field ISAR radar, the linear linear frequency modulated (LFM) signal S_T it transmits can be described in the complex model as

$$S_T\left(t\right) = \mathrm{rect}\left(\frac{t}{T_p}\right)\exp\left(\mathrm{j}2\pi\left(f_c t + \frac{1}{2}\gamma t^2\right)\right), \tag{1}$$

where t is the fast time, $\mathrm{rect}\left(u\right) = \begin{cases} 1, & |u| \leqslant 1/2 \\ 0, & |u| > 1/2 \end{cases}$, f_c represents the center frequency, T_p is the pulse width, and γ is the slope of the frequency modulation. According to scattering point and quasistatic model, the target echo can be denoted as a convolution of transmitting signal and target profile in the direction of propagation [17]. Let $[r_{\min}\ r_{\max}]$ denote the observing range gate of the radar, B is the bandwidth of radar signal, and the range resolution of radar is $\Delta = c/(2B)$. The observing range gate $R_{\text{gate}} = r_{\max} - r_{\min}$ can be divided into $N = R_{\text{gate}}/\Delta$ range cells as $[r_1, r_2, \ldots, r_N]$. Let β_i denote the reflectivity distribution of scattering centers in the range cell r_i. If there exist target scatters in the range cell r_i, we have $\beta_i > 0$, otherwise $\beta_i = 0$.

Then, we can construct a dictionary $\mathbf{\Theta} = [s_1 s_2 \cdots s_N]$, and elements of the dictionary s_i are the Nyquist samples of the echo scattered by the point at the range of r_i, where

$$s_i\left(n\right) = \mathrm{rect}\left(\frac{t_n - 2r_i/c}{T_p}\right)\exp\left(\mathrm{j}2\pi\left(f_c\left(t_n - 2r_i/c\right) + \frac{1}{2}\gamma(t_n - 2r_i/c)^2\right)\right). \tag{2}$$

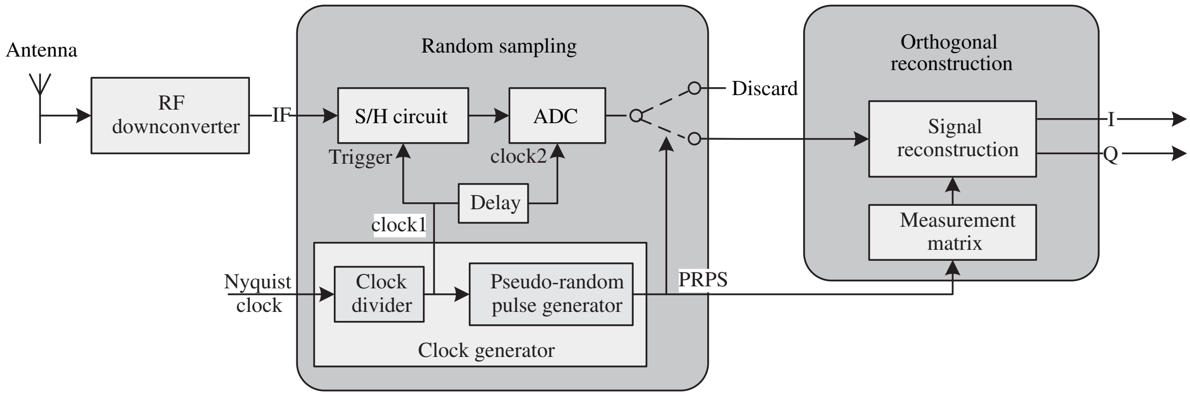

Figure 1 The block diagram of random sampling digital receiver for ISAR radar radio frequency

According to (1) and (2), we can denote the Nyquist sampling result of target echo as

$$\boldsymbol{S_r} = \boldsymbol{\Theta}\boldsymbol{\beta}, \tag{3}$$

where the $N \times 1$ column vector $\boldsymbol{\beta} = [\beta_1, \beta_2, \ldots, \beta_N]^{\mathrm{T}}$ is the digitized range profile of target and also the projection or representation of $S_R(t)$ in dictionary $\boldsymbol{\Theta}$. Generally, the dimension of target is always limited compared with the observing gate of ISAR radar, which means that only a few elements of $\boldsymbol{\beta}$ are non-zeros while others are zeros or approximate zeros. Then, we get the conclusion that the echo of target is compressible, or can be represented sparsely. The reflectivity distribution, or range profile in another word, is the sparse representation of target echo in the dictionary $\boldsymbol{\Theta}$.

3 Architecture of CS digital receiver

Based on the discussions above, the radar echo owns large bandwidth but much lower information. So, it can be efficiently captured using sub-Nyquist sampling and reconstructed afterward. We decide to use random sampling and develop a CS digital receiver for ISAR radar. A simplified block diagram of the random sampling digital receiver is shown in Figure 1.

Figure 1 shows a generic, single-channel, digital radar receiver based on CS and random sampling. It consists of a random sampling system and a CS signal processing system. The CS signal processing system is mainly implemented in software and the algorithm will be described in Section 4.

The random sampling system can be divided into three parts: sample-and-hold (SH) circuit, clock generator, and ADC. As we mentioned before, it is difficult to sample the IF signal of ISAR radar directly, so the SH circuit is a prerequisite to implementing sub-Nyquist sampling. The input bandwidth of the SH circuit is designed to cover the full spectrum of analog signal. The trigger of SH circuit is controlled by clock1 with sub-Nyquist frequency f_1, which is generated by the clock divider in Figure 1. The SH circuit captures the input signal on the rising edge of clock1 and holds it for a short time, which makes it easy to digitize the analog signal by the ADC afterward. Because of this, the requirement of sampling rate for ADC can be lower than Nyquist frequency, which will help us cut the cost and get higher resolution when selecting ADCs. The ADC in our random sampling system is driven by clock2, which owns the same frequency as clock1. Accurate delay between the two clocks is controlled specially to ensure that the output of SH settles before sampling.

After ADC, a pseudo-random pulse sequence (PRPS) controls which of these samples are collected and which are discarded. The SH circuits and ADC have accomplished sub-Nyquist sampling, and the PRPS implements random selection. The random selection is essential in CS measurement because it ensures that the measurement matrix satisfies the restricted isometry property condition of CS [8].

The clock generator is the kernel part and heartbeat of the whole system. It is driven by the Nyquist clock, which is more than two times the bandwidth of input signal. The clock1 is generated by the divider

Table 1 Contrast of ADC of different sample rates

Part No.	Sample rate (Max)	Resolution (bits)	SNR (dB)	ENOB (bits)	Approx. price (US$)
ADS62P48	210 MSPS	14	73	11.4	120.0
ADS5404	500 MSPS	12	60.8	9.8	218.75
ADC12D1000RF	2 GSPS	12	60.1	9.6	1549.45
ADC12D1600RF	3.2 GSPS	12	59	9.4	2399.46
ADC12D1800RF	3.6 GSPS	12	58.6	9.3	3299.49

with dividing factor δ_1, and the frequency of clock1 is $f_1 = f_{\mathrm{Nyquist}}/\delta_1$. The PRPS can be treated as a sequence of pulses, which is the result of random selection from the pulses of clock1. The random selecting factor is δ_2, which means only $1/\delta_2$ of the input samples are collected while others are ignored. The PRPS must be able to retrieve, because it is crucial to the CS reconstruction. For flexibility in implementing and testing, the PRPS pattern can be set by a repeating pseudo-random bit sequence provided by an external ROM.

In the random sampling system presented above, the actual sampling rate is reduced in two steps. First, the SH circuit reduces the frequency of signal of interest to be f_1. Second, the random selection discards parts of the samples and reduces the sampling rate equivalently. The compression ratio depends on both δ_1 and δ_2. δ_1 defines the limit of sampling rate and δ_2 reduces the total amount of final samples.

Suppose the radar transmits LFM signal with bandwidth of 1 GHz and pulse width of 300 µs, the center frequency of IF signal is 2.4 GHz. If a traditional IF digital receiver is designed for this radar, the input bandwidth of ADC must be at least 2.9 GHz and sample rates must be 2.4 GSPS. According to the current development of ADC, only a few expensive and high-speed ADCs can satisfy these requirements. If we use such ADCs to digitize the echo signal, the length of samples for one pulse is $N_1 = f_s\,(T_p + r_{\mathrm{gate}}/c)$. Let the sample rate $f_s = 2.4$ GSPS, the range gate $r_{\mathrm{gate}} = 50$ m, then we will have $N_1 = 720400$. It is a pretty huge number and much larger than the information level of the radar echo signal. In our digital receiver based on random sampling, the sample rate of ADC is determined by the complexity of the target range profile, not the bandwidth of the signal. For the radar mentioned in this section, if we set the division factor of clock divider as $\delta_1 = 10$, the requirement of sampling speed will be reduced to $f_{\mathrm{sample}} \geqslant f_{\mathrm{Nyquist}}/\delta_1 = 200$ MHz. So, an ADC with sample rate more than 200 MHz will satisfy our demand. In most applications of ADCs, lower sampling speed gives the engineers more options in choosing ADCs and better performance. Table 1 shows the parameters and prices of some typical state-of-the-art ADCs, which can be found from the official website of Texas Instruments. From Table 1, we can see that it is more and more difficult and expensive to achieve better performance like resolution and signal noise ratio (SNR), when the sampling speed of ADC becomes higher. Using random sub-Nyquist sampling, we can implement equivalent sampling with much lower sampling rate, thus higher digitizing resolution, higher ENOB, and better SNR will be available at even less price. This will surely not only help cut the cost of digital receiver but also bring more benefits to the digital signal processing afterward.

4 Algorithm for orthogonal reconstruction

Using CS digital receiver, we can obtain sub-Nyquist samples of radar echoes, but it is not the complete solution for our problem. The next question is how to reconstruct the information of interest from these samples. The amount of samples is much less than conventional digital receiver, but the subsampled echoes are also insufficient for conventional signal processing, such as matched filtering and ISAR imaging.

4.1 Orthogonal digital downconverter in conventional radar system

Complex signal, also called quadrature signal, is used in many fields of science and engineering and is necessary to describe the processing and implementation that takes place in modern digital systems [18]. In radar system, complex signal is very convenient for coherent signal processing. However, in the real

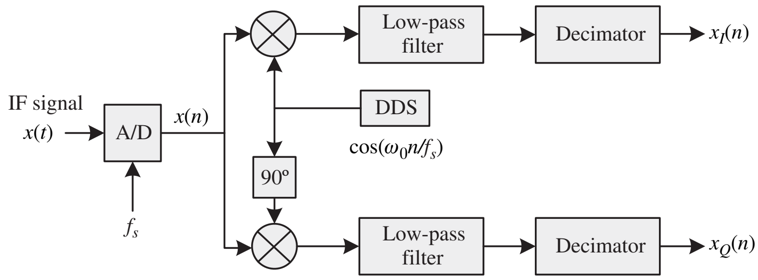

Figure 2 The block diagram of DDC in conventional digital radar receiver.

world all physical signals and waveforms are real-valued, and the radar antenna can only transmit and receive real signal, which is the real part of complex signal.

As a result, in-phase/quadrature demodulation is always one of the most elementary parts in the radar receiver, no matter in analog receiver or digital one [19]. In conventional digital radar receiver, digital down converter (DDC) converts the digitized IF signal samples to complex baseband signal. Figure 2 shows the architecture of direct DDC in conventional digital radar receiver [20]. The analog IF signal is first sampled by an ADC, and all of the subsequent processing, such as spectral multiplication, low-pass filtering, and decimating, are done digitally. The DDC has been proved to have better performance of coherent processing than analog one [21,22].

The DDC can realize the orthogonal demodulation in digital receiver which uses Nyquist or band-pass sampling, but when we try to employ CS to subsample the radar echoes, the DDC will not be effective for the nonuniform sampled data. Because the frequency spectrum of the signal will be destroyed and aliased after the sub-Nyquist sampling, the low-pass filter in DDC cannot function correctly anymore. So in our CS digital receiver, we cannot use the conventional DDC to convert the real signal to complex anymore.

4.2 Orthogonal reconstructing algorithm for CS digital receiver

To reconstruct complex signal from subsampled radar echoes, we need to solve this problem in CS method and build a dictionary or basis for the real-valued radar echo first. In Section 2, we have built a complex-valued model for the sparse representation of ISAR radar echoes. Considering that only real-valued signal exists in the real world, the real echo that the digital receiver receives shall be denoted as

$$\boldsymbol{S}_{\boldsymbol{r}}' = \Re\{\boldsymbol{S}_{\boldsymbol{r}}\} = \Re\{\boldsymbol{\Theta}\boldsymbol{\beta}\}, \tag{4}$$

where $\Re\{\cdot\}$ is the real operator, which obtains the real part of complex expression. As can be seen, the process of random sampling can be expressed in matrix form:

$$\boldsymbol{y} = \boldsymbol{\Phi}\mathbf{S}_{\boldsymbol{r}}' = \boldsymbol{\Phi}\cdot\Re\{\boldsymbol{\Theta}\beta\} = \Re\{\boldsymbol{\Phi}\boldsymbol{\Theta}\beta\}, \tag{5}$$

where both $\boldsymbol{\Theta}$ and $\boldsymbol{\beta}$ are complex. The random measuring matrix $\boldsymbol{\Phi}$ is real-valued and can be obtained by randomly selecting rows from the identify matrix $\mathbf{I}$.

For most of the CS algorithms, the measured signal and the measuring matrix are either both real-valued or complex-valued [23–26]. They cannot be used to solve our problem of reconstructing complex signal from real-valued measurements. Here, we propose an orthogonal reconstructing algorithm to compile with our CS digital receiver.

To reconstruct the complex-valued range profile from random sampled echo, let us suppose a complex-valued matrix $\boldsymbol{\Psi} = \boldsymbol{\Phi}\boldsymbol{\Theta}$, and let $\Im\{\cdot\}$ denote the imaginary operator. We can change (5) to another expression as follows:

$$\boldsymbol{y} = \Re\{\boldsymbol{\Psi}\beta\} = \begin{bmatrix} \Re\{\boldsymbol{\Psi}\} & \Im\{\boldsymbol{\Psi}\} \end{bmatrix} \cdot \begin{bmatrix} \Re\{\boldsymbol{\beta}\} \\ -\Im\{\boldsymbol{\beta}\} \end{bmatrix}. \tag{6}$$

Let $\boldsymbol{\Psi}' = \begin{bmatrix} \Re\{\boldsymbol{\Psi}\} & \Im\{\boldsymbol{\Psi}\} \end{bmatrix}$ and $\boldsymbol{\beta}' = \begin{bmatrix} \Re\{\boldsymbol{\beta}\} \\ -\Im\{\boldsymbol{\beta}\} \end{bmatrix}$, so the process of random sampling can be written in a real-valued matrix form as $\boldsymbol{y} = \boldsymbol{\Psi}'\boldsymbol{\beta}'$, where $\boldsymbol{\beta}'$ is a sparse vector and $\boldsymbol{\Psi}'$ can be treated as a new compressed measurement matrix. According to the theory of CS, we can reconstruct $\boldsymbol{\beta}'$ by solving the optimization problem:

$$\widehat{\boldsymbol{\beta}'} = \min \|\boldsymbol{\beta}'\|_0 \text{ s.t. } \boldsymbol{y} = \boldsymbol{\Psi}'\boldsymbol{\beta}'. \tag{7}$$

If we consider the noise during measuring, then the optimization problem can be changed into

$$\widehat{\boldsymbol{\beta}'} = \min \|\boldsymbol{\beta}'\|_0 \text{ s.t. } \|\boldsymbol{y} - \boldsymbol{\Psi}'\boldsymbol{\beta}'\|_2^2 < \varepsilon. \tag{8}$$

According to (7) and (8), we have converted the processing of orthogonal receiver and matched filter into a CS reconstructing problem, and all the algorithms that are proposed for real-valued CS can be used to solve our problem.

Some effective CS optimization algorithms have been presented to solve problem like (8), such as orthogonal matching pursuit (OMP), ℓ_1 optimization algorithm, and Bayesian algorithm [23–25]. The smooth ℓ_0 (SL0) method proposed by Mohimani et al. [26] has a good trade-off between accuracy and complexity. Compared with OMP and ℓ_1 optimization algorithm, the SL0 does not need prior information about sparsity level of original signal. So, it is very suitable for the application in radar digital receiver, since the structure of target is always unknown before the range profiles are reconstructed.

By solving (8), we can obtain the real and image parts of target profile at the same time from the subsampled real-valued echo. As a result, our proposed design and algorithm can simplify the architecture of digital receiver and the flow of radar signal processing.

5 Experimental results

In this section, we provide some simulation results to verify the effectiveness of the proposed CS digital receiver and orthogonal reconstructing algorithm.

5.1 Simulated data analysis

Suppose the radar transmits LFM signal with bandwidth $B = 1$ GHz, center frequency $f_c = 2.4$ GHz, pulse repetition frequency $f_{\text{prf}} = 1000$ Hz, and the pulse width $T_p = 300$ μs. In the conventional digital receiver using band-pass sampling, the sampling frequency of ADC should be at least 2 GHz, and we choose $f_s = 2.4$ GSPS. Let the range of target be 10000 m, and the reflectivity distribution of target is shown in Figure 3(a). The radar echoes are generated according to the point scattering model. For simplicity, suppose the translational velocity during the CPI is zero, so the target can be treated as a simple rotating platform. The rotating angular velocity is 0.4 rad/s, so the rotating angular of 256 consecutive pulses will be appropriate for ISAR imaging.

From the parameters, we can calculate the range resolution as $\Delta_r = C/2B = 0.15$ m. Let the range gate be 20 m, and if we employ conventional digital receiver using band-pass Nyquist sampling, we will get one echo with length of $N = 720320$. Define the compression ratio of measurement in fast time as $N/M = 50$ by setting $\delta_1 = 5$ and $\delta_2 = 10$. So, the equivalent sampling rate in CS digital receiver is only 45 MHz, and the length of sampled echo will be $M = 14406$. It is obvious that the CS digital receiver can reduce the sampling rate and the amount of sampled data.

In the following simulation, we try to reconstruct the range profiles from subsampled echoes. The performance of our proposed orthogonal reconstructing algorithm is compared with conventional CS method. Figure 4 shows the range profile reconstructed from one subsampled echo. Figure 4(a) is the result of the conventional CS method based on real-valued sparse dictionary, and Figure 4(b) is obtained using our orthogonal method. As we can see, the reconstructed result of our orthogonal method consists of both real and image parts of complex-valued range profile, while the conventional method can only get the real part.

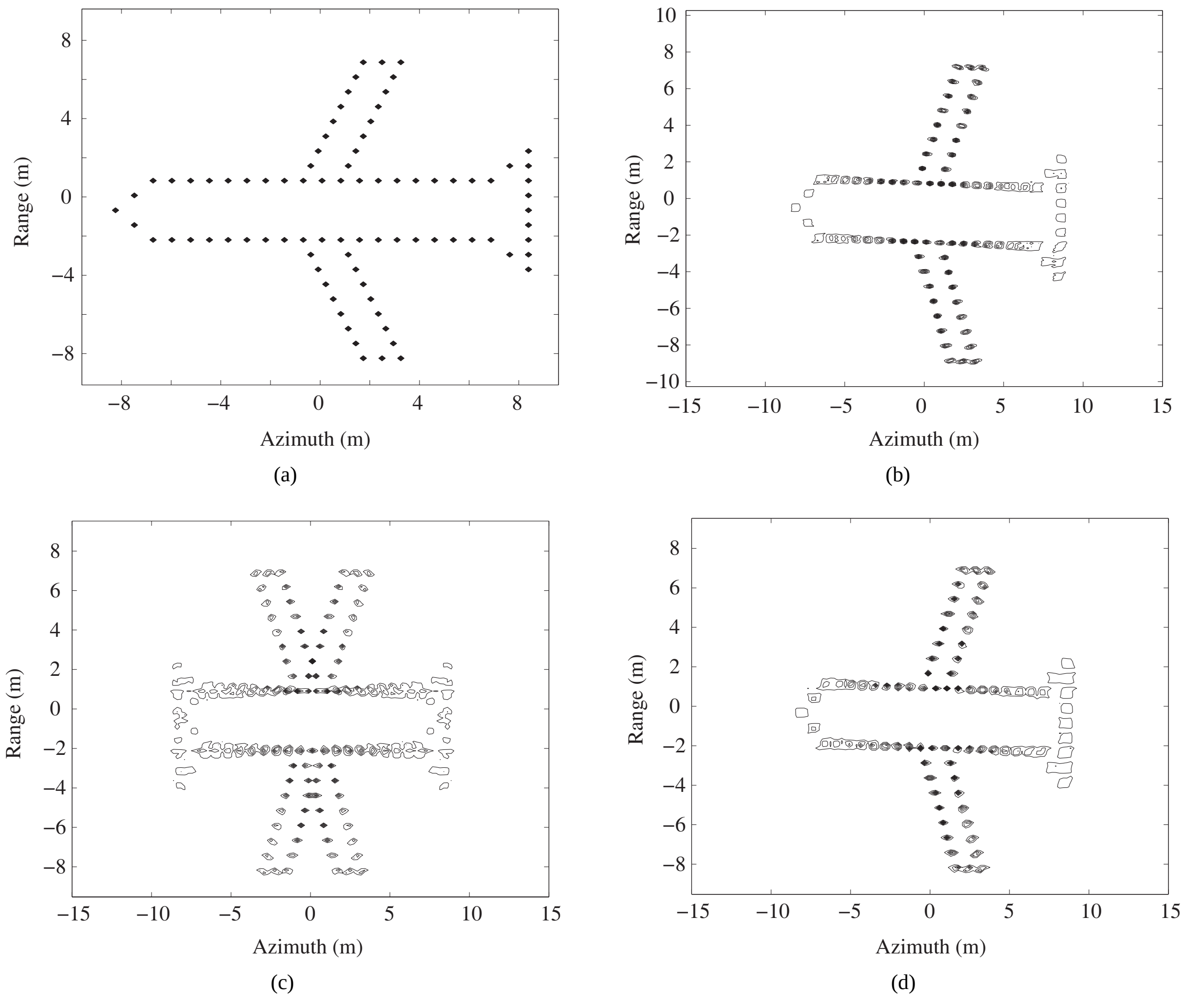

Figure 3 (a) Reflectivity distribution of simulated target; (b) ISAR imaging result using conventional range-Doppler method; (c) image reconstructed using conventional CS method and (d) image reconstructed using our orthogonal CS method.

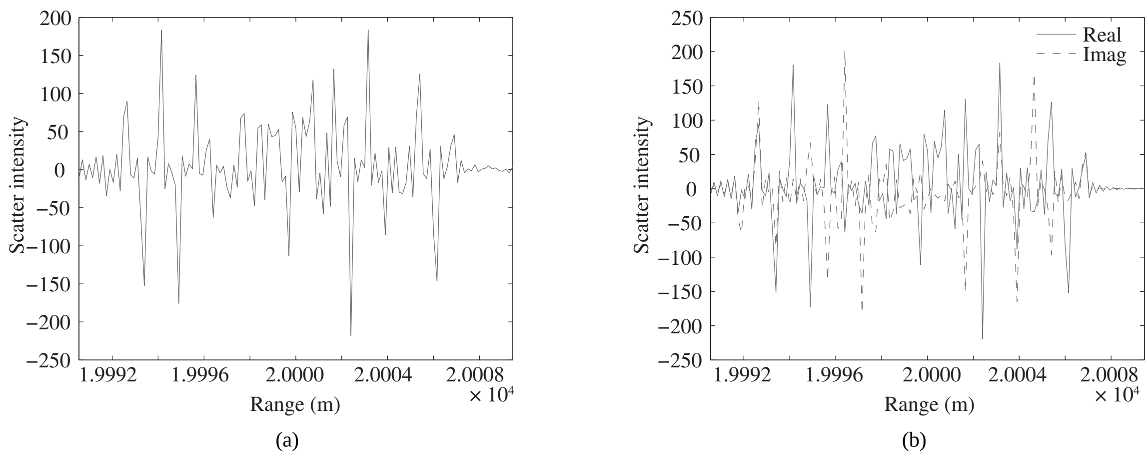

Figure 4 Comparison of range profiles reconstructed from different CS methods. (a) Range profile reconstructed using conventional CS method and (b) range profile reconstructed using our proposed orthogonal CS method.

Then, we reconstruct 256 consecutive echoes of the target and use the range-Doppler algorithm to generate the ISAR imaging result. Figure 3(b) is the result using the whole Nyquist sampled echoes.

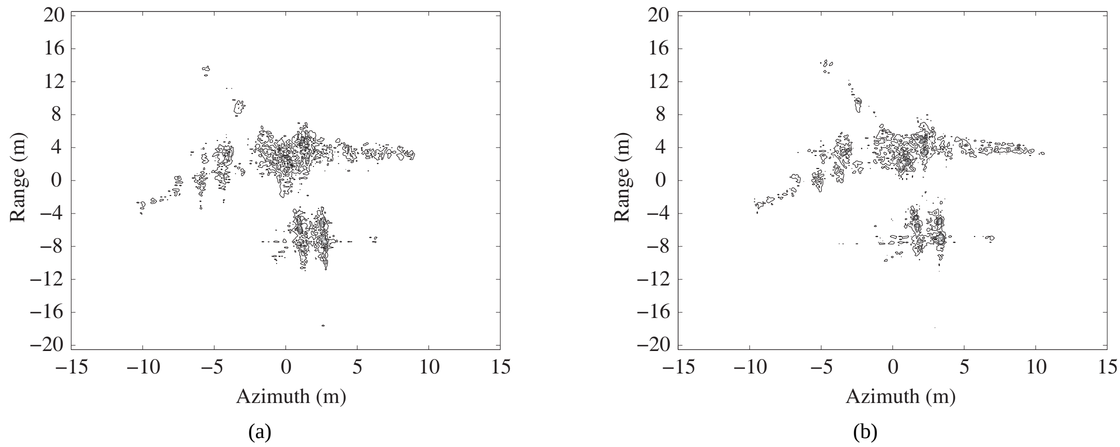

Figure 5 Comparison of imaging results using actual measured data. (a) Imaging result using whole original echoes and (b) reconstructed image using subsampled echoes at 1/100 of Nyquist sampling rate.

Figure 3(c) is the imaging result based on conventional CS algorithm, where the sparse basis and the reconstructed range profiles are real-valued. The result proves that complex-valued range profiles and the phase information are essential for ISAR imaging. Using only real parts of range profiles, the aliasing in azimuth domain is unavoidable. Figure 3(d) is the result of our proposed orthogonal reconstruction, which shows that the phase information of range profiles is preserved perfectly after the reconstruction using orthogonal reconstructing algorithm. By the comparisons in Figures 3 and 4, we can come to a conclusion that the architecture of CS digital receiver and the orthogonal reconstructing algorithm proposed in this paper are feasible for ISAR radar.

5.2 Measured data analysis

Some actual measured data sets are also used to test the orthogonal CS algorithm. The raw data were acquired and recorded using an experimental ISAR radar with bandwidth $B = 1$ GHz, and the target is a flying civilian aircraft. The raw data were sampled at Nyquist speed by an existing digital receiver using band-pass sampling and are real-valued without processing by DDC. As a demonstration, we simulate the process of random sampling by randomly selecting some data points from the measured raw data. The original length of echo is $N = 4800000$ in one pulse. We set $\delta_1 = 10$ and $\delta_2 = 10$ in the random sampling, and the compressed ratio $N/M = 100$, thus we get subsampled echoes with length of M = 48000. After reconstruction using orthogonal CS method, we get the complex range profiles, and then the ISAR image is obtained using range-Doppler imaging method. The imaging result in Figure 5(a) is obtained using the whole original Nyquist-sampled echoes, while Figure 5(b) is reconstructed from the randomly sampled echoes using orthogonal CS method.

The entropy of image is usually used to evaluate the quality of ISAR images, thus we calculate the entropy of two images. The entropies of range-Doppler imaging result and CS reconstructed result are $E_1 = 8.409$ and $E_2 = 9.04$, respectively. Although the quality of reconstructed image is a little worse than RD image, this is still receivable and pretty amazing considering the large compressed ratio and much less data required by CS method.

To study the effect of reconstructing method with different compressed ratios, a series of experiments are carried on with different sets of compression ratios. The images are achieved using the same ISAR imaging algorithms, and we use the entropy of the ISAR image to evaluate the quality of reconstruction. Smaller entropy means higher quality of imaging and better performance of reconstruction of range profiles. Figure 6 shows the comparison of images' entropy in different compression ratios. The reconstructing algorithm is implemented in Matlab codes and runs on a PC with Intel(R) Core(TM) i5-3740 @3.2 GHz CPU and 8 GB memory. The computational time consumption of reconstructing images under different compression ratios is presented in Figure 7.

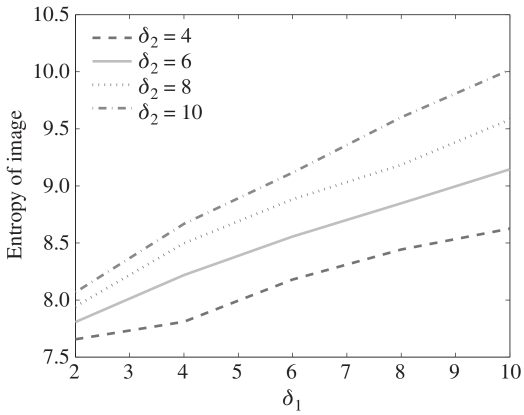

Figure 6 Entropy of reconstructed images under different compression ratios.

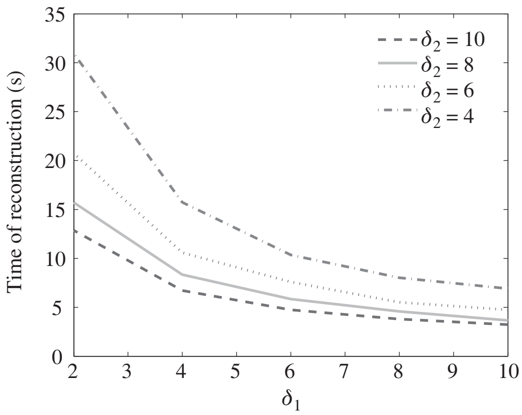

Figure 7 Time consumption of reconstructing images under different compression ratios.

As we can see, although the sampling rate and amount of samples are both reduced obviously by random sampling, we can still get imaging result using orthogonal reconstruction. The performance of reconstructing algorithm gets worse as the compression ratio becomes large, but the computational time consumption decreases at the same time. This is consistent with the theoretical analysis and a very common contradictory in CS. As a result, appropriate trade-off must be made between the compression ratio and difficulty in implementation, which depends on the actual demand in practical application.

6 Conclusion and future work

In this paper, a novel structure of CS digital receiver is proposed for wideband ISAR radar. Random sampling is implemented to digitalize the ultra wideband signal using ADC of lower sampling speed and limited input bandwidth. Compared with the conventional digital receiver, our design can remarkably reduce the amount of data needed to obtain high-resolution range profiles. A sparse representation for the radar echo signal based on the point scattering model is analyzed in this paper. An orthogonal reconstructing method is proposed to reconstruct the complex-valued range profiles of target for ISAR radar. Using the sparse basis and SL0 reconstructing algorithm, we can directly obtain the range profiles from subsampled echoes, and the processes of down converter and matched filtering are directly realized during the reconstruction. Although the analysis of CS digital receiver in this paper is based on ISAR radar, we believe the architecture will also be effective and helpful in other wideband radars. The results of analysis in both simulated and measured data have proved the feasibility of our design and reconstructing method. This paper mainly focuses on the methodology and system design of CS digital receiver for ISAR radar. More research about details of implementation of hardware and algorithm will be discussed in future work.

Acknowledgements

This work was supported by National Natural Science Foundation of China (Grant No. 61002025).

References

1 Mitola J. The software radio architecture. IEEE Commun Mag, 1995, 33: 26–38
2 Wu Y, Li J. The design of digital radar receiver. IEEE Aes Mag, 1998, 35: 35–41
3 Hasan S M, Lutfi A. A low-cost high-performance digtial radar test bed. IEEE Trans Instrum Meas, 2013, 62: 221–229
4 Pekau H, Haslett J W. A comparison of analog front end architectures for digital receivers. In: Canadian Conference on Electrical and Computer Engineering, Saskatoon, 2005. 1073–1077

5 Vaughan R G, Scott N L, White D R. The theory of bandpass sampling. IEEE Transn Signal Process, 1991, 39: 1973–1991

6 Wiley C A. Synthetic aperture radars. IEEE Trans Aerosp Electron Syst. 1985, 21: 440–443

7 Zhou F, Bai X R, Xing M D, et al. Analysis of wide-angle radar imaging. IET Proc-Radar Sonar Navig, 2011, 5: 449–457

8 Donoho D L. Compressed sensing. IEEE Trans Inf Theory, 2006, 52: 1289–1306

9 Tropp J A, Laska J N, Duarte M F, et al. Beyond Nyquist: efficient sampling of sparse bandlimited signals. IEEE Trans Inf Theory, 2010, 56: 520–544

10 Zhang B C, Hong W, Wu Y R. Sparse microwave imaging: principles and applications. Sci China Inf Sci, 2012, 55: 1722–1754

11 Baraniuk R, Steeghs P. Compressive radar imaging. In: Proceedings of IEEE Radar Conference, Boston, 2007. 128–133

12 Potter L C, Ertin E, Parker J T. Sparsity and compressed sensing in radar imaging. Proc IEEE, 2010, 98: 1006–1020

13 Wang H X, Liang Y, Xing M D, et al. ISAR imaging via sparse frequency-stepped chirp signal. Sci China Inf Sci, 2012, 55: 877–888

14 Bai X R, Zhou F, Xing M D, et al. High-resolution radar imaging of air targets from sparse azimuth data. IEEE Trans Aerosp Elect Syst, 2012, 48: 1643–1655

15 Ender J H G. On compressive sensing applied to radar. Signal Process, 2010, 90: 1402–1414

16 Zhu F, Zhang Q, Luo Y, et al. A novel cognitive ISAR imaging method with random stepped frequency chirp signal. Sci China Inf Sci, 2012, 55: 1910–1924

17 Wu C, Liu K Y, Jin M. Modeling and a correlation algorithm for spaceborne SAR signals. IEEE Trans Aerosp Electron Syst, 1982, 18: 563–574

18 Martin K W. Complex signal processing is not complex. IEEE Trans Circ Syst, 2004, 51: 1823–1836

19 Fudge J, Legako M, Sehreiner C. An approach to efficient wideband digital down conversion. In: Proceedings of International Conference on Signal Processing Applications and Technology, Toronto, 1998. 713–717

20 Hentschel T, Henker M, Fettweis G. The digital front-end of software radio terminals. IEEE Pers Commun, 1999, 6: 40–46

21 Lohning M, Hentschel T, Fettweis G. Digital down conversion in software radio terminals. In: Proceedings of 10th European Signal Processing Conference, Tampere, 2000. 1517–1520

22 Jantzi S A, Martin K, Sedra A S. Quadrature bandpass sigma-delta modulation for digital radio. IEEE J Solid-State Circuits, 1997, 32: 1935–1949

23 Lei J. Generalized reconstruction algorithm for compressed sensing. Comput Elec Eng, 2011, 37: 570–588

24 Mileounis G, Babadi B, Kalouptsidis N, et al. An adaptive greedy algorithm with application to nonlinear communications. IEEE Trans Signal Process, 2010, 58: 2998–3007

25 Ji S, Xue Y, Carin L. Bayesian compressive sensing. IEEE Trans Signal Process, 2008, 56: 2346–2356

26 Mohimani H, Babaie-Zadeh M, Jutten C. A fast approach for overcomplete sparse decomposition based on smoothed ℓ^0 norm. IEEE Trans Signal Process, 2009, 57: 289–301